KI REPORTS
KIReports.org
CLINICAL RESEARCH

Germline Mutations for Kidney Volume in ADPKD

Hiroshi Kataoka[1,2], Rie Yoshida[1], Naomi Iwasa[1], Masayo Sato[1], Shun Manabe[1], Keiko Kawachi[1], Shiho Makabe[1], Taro Akihisa[1], Yusuke Ushio[1], Atsuko Teraoka[1], Ken Tsuchiya[3], Kosaku Nitta[1] and Toshio Mochizuki[1,2]

[1]Department of Nephrology, Tokyo Women's Medical University, Tokyo, Japan; [2]Clinical Research Division for Polycystic Kidney Disease, Department of Nephrology, Tokyo Women's Medical University, Tokyo, Japan; and [3]Department of Blood Purification, Tokyo Women's Medical University, Tokyo, Japan

Introduction: Valid prediction models or predictors of disease progression in children and young patients with autosomal dominant polycystic kidney disease (ADPKD) are lacking. Although total kidney volume (TKV) and Mayo imaging classification are generally used to predict disease progression in patients with ADPKD, it remains unclear whether germline mutation types are associated with these factors. We therefore investigated the association between mutation type and TKV and Mayo imaging classification among patients with ADPKD.

Methods: A total of 129 patients with ADPKD who underwent genetic analyses were enrolled in the study. The associations between the severity of PKD (TKV $\geq$ 1000 ml and Mayo classes 1C–1E) and the *PKD1* mutation types (nonsense mutation, frameshift or splicing mutation, and substitution) were evaluated.

Results: Among the mutation types, only *PKD1* splicing/frameshift mutation had significant associations with TKV $\geq$ 1000 ml in sex-adjusted and multivariable logistic analyses. Similarly, only the *PKD1* splicing/frameshift mutation was significantly associated with Mayo 1C–1E in sex-adjusted and multivariable logistic analyses. *PKD1* nonsense mutation, *PKD1* substitution, or *PKD1* mutation position had no significant association with TKV $\geq$ 1000 ml or Mayo 1C–1E.

Conclusion: Kidney cyst severity differs according to the mutation types in *PKD1*. Patients with *PKD1* splicing mutations or *PKD1* frameshift mutations are associated with TKV $\geq$ 1000 ml or Mayo 1C–1E. Detailed assessment of mutation types may be useful for predicting renal prognosis in patients with ADPKD and may especially contribute to the care of a high-risk group of children with ADPKD.

Kidney Int Rep (2022) **7,** 537–546; https://doi.org/10.1016/j.ekir.2021.12.012
KEYWORDS: autosomal dominant polycystic kidney disease; frameshift mutation; germline mutation; kidney volume; Mayo imaging classification; splicing mutation

ADPKD is the most common progressive hereditary kidney disease.[1] At present, kidney disease progression in patients with ADPKD is generally predicted using estimated glomerular filtration rate (eGFR),[2,3] TKV,[4–6] and the Mayo imaging classification.[7–9] eGFR, as a representative predictor of chronic kidney disease, is strong but less sensitive in the early stages of ADPKD because the eGFR sometimes declines in a nonlinear pattern[10] and generally remains in the normal range (eGFR $\geq$ 90 ml/min per 1.73 m^2) before the age of 30 years, despite the progressive formation of cysts.[4] Therefore, in early stage disease, kidney volume has been used as a predictor[5,7,11,12] and has already been used as the end point in clinical trials.[13] Perrone *et al.*[5] reported that the risk of progression to a 30% decline in eGFR or end-stage renal disease in patients with a larger TKV of $\geq$1000 ml was significantly greater than that in patients with a smaller TKV (<1000 ml), regardless of kidney function. The Mayo imaging classification divides typical ADPKD into 5 groups (Mayo image classes 1A–1E) according to age- and height-adjusted TKV to predict renal outcome.[7] Patients with Mayo image classes 1C–1E (Mayo 1C–1E) had a faster decline in renal function compared with those with classes 1A–1B[7]; Mayo image classes 1C–1E are defined as "rapidly progressing disease," and for which, tolvaptan treatments are recommended.[8,9]

Correspondence: Toshio Mochizuki, Clinical Research Division for Polycystic Kidney Disease, Department of Nephrology, Tokyo Women's Medical University, 8-1 Kawada-cho, Shinjuku-ku, Tokyo 162-8666, Japan. E-mail: mtoshi@twmu.ac.jp

Received 10 November 2021; accepted 6 December 2021; published online 13 December 2021

Although TKV and the Mayo imaging classification are clinically important, valid prediction models to identify children with ADPKD who therefore likely to suffer kidney failure are still lacking, as the radiological features in children are different from those in adult patients.[14] As TKV changes with aging, the Mayo imaging classification is only applicable from 16 years of age.[7] This situation is unfavorable because 20% of children with ADPKD have hypertension,[15] and the pediatric stages of ADPKD have been recognized as important stages for disease understanding and treatment.[14] Considering that beneficial effects of early treatment for slowing the increase in TKV have been reported in children with ADPKD[16] and that valid prediction models to identify children with ADPKD likely to suffer kidney failure are lacking,[14] it is important to identify a high-risk group among patients with ADPKD, who are candidates for early intervention. The lack of early prognostic markers for kidney prognosis is still a concern for both physicians and patients[17]; additional indicators other than eGFR, TKV, and Mayo 1C–1E are clinically desired in children with ADPKD.

Mutations in *PKD1* and *PKD2* are responsible for ADPKD.[18,19] We believe that detailed information on germline mutations could be helpful in predicting the severity of ADPKD. Indeed, many reports have indicated that patients with a *PKD1* mutation, especially truncating mutations, have a faster decline in kidney function than patients with a *PKD2* mutation.[20–25] Similarly, patients with *PKD1* mutations, especially truncating mutations, have significantly larger kidneys[26–28] and more cysts[26] than those with *PKD2* mutations. As a result, genotypic factors such as truncating *PKD1* mutations, nontruncating *PKD1* mutations, and *PKD2* mutations have been adopted in scoring systems (PROPKD Score) to predict kidney failure.[29] Although the PROPKD Score contributes to the clinical setting, it has limited value in patients who are <35 years old and who do not have complications.[30] In addition, the genetic variables used in the PROPKD Score are limited to only 3 mutation types (truncating *PKD1*, nontruncating *PKD1*, and *PKD2*). Therefore, useful genetic information for determining the prognosis of a patient is yet to be determined. In ADPKD, 4 mutation types (splicing mutation, frameshift mutation, nonsense mutation, and substitution) are reported to account for >90% of patients.[30,31] Of these gene mutations, 3 (splicing mutations, frameshift mutations, and nonsense mutations) are classified as truncating mutations, but they have recently been reported to have different effects on disease severity in patients with ADPKD.[32,33] In particular, eGFR decline is reported to be associated with *PKD1* splicing mutations and *PKD1* frameshift mutations.[33] At present, the relationship between TKV ≥ 1000 ml, Mayo imaging classification of 1C–1E, and detailed gene mutation types in *PKD* has not been reported. In this study, we hypothesized that *PKD1* splicing and frameshift mutations could be predictors for a TKV ≥ 1000 ml and Mayo imaging class of 1C–1E; in addition, we investigated the relationship between these 2 predictors and the detailed gene mutation types.

METHODS

Study Design

A total of 129 patients with ADPKD who presented at the Kidney Center at the Tokyo Women's Medical University Hospital (Tokyo, Japan) and underwent genetic analysis[34] between 2003 and 2017, including magnetic resonance imaging or computed tomography to evaluate TKV and Mayo imaging classification, were included in the study (Supplementary Figure S1). All procedures were approved by the research ethics committee of Tokyo Women's Medical University (number 196 B) in accordance with the 1964 Declaration of Helsinki and its later amendments or with comparable ethical standards. Written informed consent was obtained from all the participants. A detailed description of the methods can be found in the Supplementary Material (Supplementary Methods: mutation analysis, measurement of kidney volume and kidney cyst, definition of comorbidities). The participants were assessed up to October 31, 2020.

Outcome Evaluation

The primary outcomes were TKV ≥ 1000 ml and Mayo imaging classification 1C–1E.

Statistical Analyses

Continuous variables are reported as mean ± SD or as median (minimum, maximum). Categorical variables are reported as percentages, unless otherwise stated. Group differences were evaluated using unpaired *t* tests, Mann-Whitney *U* tests, χ^2 tests, or Fisher exact tests, as appropriate. Logistic regression analyses were performed to determine the factors associated with outcomes.[35,36] Variables of interest, including general risk factors for outcomes based on existing knowledge, were included in the multivariable model. Standard methods were applied to estimate sample size for multivariable logistic regression, with at least 5 outcomes needed for each independent variable.[36] Discriminatory ability was measured using the area under the receiver operating characteristic curve. The goodness-of-fit was evaluated using McFadden's pseudo-*R*-squared (pseudo-R^2).[37] All statistical tests were 2-tailed, and statistical significance was set at $P <$

Table 1. Patient characteristics according to TKV and Mayo classification (entire cohort, $N = 129$)

Variables	Total, $N = 129$	Patients with TKV <1000 ml, $n = 55$	Patients with TKV ≥1000 ml, $n = 74$	*P* value	Total, $N = 121$	Mayo imaging classification 1A–1B, $n = 48$	Mayo imaging classification 1C–1E, $n = 73$	*P* value
Clinical findings								
Age (yr)	45 (15–77) [129]	43 (15–74)	47 (22–77)	0.0709	45 (15–77) [121]	50.5 (21–77)	44 (15–75)	0.0019[a]
Sex (men), *n* (%)	55 (42.6) [129]	14 (25.5)	41 (55.4)	0.0007[a]	52 (43.0) [121]	15 (31.3)	37 (50.7)	0.0346[a]
Smoking, current or former, *n* (%)	32 (24.8) [129]	9 (16.4)	23 (31.1)	0.0556	31 (25.6) [121]	8 (16.7)	23 (31.5)	0.0673
PKD1/*PKD2*/unknown, *n* (%)	99 (76.7)/21 (16.3)/9 (7.0) [129]	42 (76.4)/8 (14.6)/5 (9.1)	57 (77.0)/13 (17.6)/4 (5.4)	0.6726	93 (76.9)/21 (17.4)/7 (5.8) [121]	34 (70.8)/10 (20.8)/4 (8.3)	59 (80.8)/11 (15.1)/3 (4.1)	0.4018
PKD1 truncating mutation, *n* (%)	68 (52.7) [129]	25 (45.5)	43 (58.1)	0.1546	63 (52.1) [121]	21 (43.8)	42 (57.5)	0.1376
PKD1 splicing mutation or frameshift mutation, *n* (%)	34 (26.4) [129]	8 (14.6)	26 (35.1)	0.0087[a]	33 (27.3) [121]	7 (14.6)	26 (35.6)	0.0110[a]
PKD1 nonsense mutation, *n* (%)	29 (22.5) [129]	13 (23.6)	16 (21.6)	0.7863	27 (22.3) [121]	11 (22.9)	16 (21.9)	0.8973
PKD1 substitution, *n* (%)	28 (21.7) [129]	14 (25.5)	14 (18.9)	0.3732	27 (22.3) [121]	11 (22.9)	16 (21.9)	0.8973
PKD1 mutation position (cDNA)	7816 (1–12,721) [99]	7546 (1–12,577)	8309 (529–12,721)	0.0834	8068 (1–12,721) [93]	7546 (1–12,145)	8515 (529–12,721)	0.0665
PKD2 mutation position (cDNA)	1249 (1–2614) [19]	1249 (181–2614)	1249 (1–2507)	0.5497	1249 (1–2614) [19]	1249 (181–2614)	1249 (1–2507)	0.5589
CKD1–2/CKD3/CKD4–5, *n* (%)	50 (39.4)/45 (35.4)/32 (25.2) [127]	33 (60.0)/16 (29.1)/6 (10.9)	17 (23.6)/29 (40.3)/26 (36.1)	<0.0001[a]	48 (39.7)/41 (33.9)/32 (26.5) [121]	21 (43.8)/18 (37.5)/9 (18.8)	27 (37.0)/23 (31.5)/23 (31.5)	0.2978
Mayo imaging classification class 1A–1B/ class 1C–1E, *n* (%)	48 (39.7)/73 (60.3) [121]	38 (76.0)/12 (24.0)	10 (14.1)/61 (85.9)	<0.0001[a]	NA	NA	NA	NA
eGFR (ml/min per 1.73m^2)	52.2 ± 29.4 [127]	66.9 ± 26.4	41.0 ± 26.7	<0.0001[a]	52.0 ± 29.7 [121]	56.9 ± 27.7	48.7 ± 30.7	0.1384
U-Prot (g/g·Cre)	0.00 (0.00–7.14) [104]	0.00 (0.00–0.59)	0.08 (0.00–7.14)	0.0059[a]	0.00 (0.00–7.14) [99]	0.00 (0.00–7.14)	0.00 (0.00–1.76)	0.2151
TKV (ml)	1525.0 ± 1161.1 [129]	665.1 ± 195.1	2164.1 ± 1168.1	<0.0001[a]	1532.7 ± 1154.6 [121]	765.6 ± 369.5	2037.0 ± 1217.6	<0.0001[a]
TKV ≥1000 ml, *n* (%)	74 (57.4) [129]	NA	NA	NA	71 (58.7) [121]	10 (20.8)	61 (83.6)	<0.0001[a]
htTKV (ml/m)	923.2 ± 677.3 [121]	410.9 ± 122.1	1283.9 ± 675.6	<0.0001[a]	923.2 ± 677.3 [121]	472.5 ± 223.6	1219.5 ± 712.3	<0.0001[a]
Maximum kidney cyst diameter (cm)	6.54 ± 2.09 [129]	5.54 ± 2.03	7.28 ± 1.82	<0.0001[a]	6.56 ± 2.04 [121]	5.66 ± 1.94	7.15 ± 1.89	<0.0001[a]
Maximum liver cyst diameter (cm)	3.95 ± 3.55 [129]	3.63 ± 3.21	4.18 ± 4.79	0.3905	3.80 ± 3.49 [121]	3.87 ± 3.30	3.76 ± 3.64	0.8627
Intracranial aneurysm, *n* (%)	19 (14.7) [129]	2 (3.6)	17 (23.0)	0.0021[a]	19 (15.7) [121]	3 (6.3)	16 (21.9)	0.0224[a]
Comorbidities								
Hypertension, *n* (%)	81 (62.8) [129]	23 (41.8)	58 (78.4)	<0.0001[a]	79 (65.3) [121]	25 (52.1)	54 (74.0)	0.0133[a]
Hyperuricemia, *n* (%)	44 (34.1) [129]	9 (16.4)	35 (47.3)	0.0002[a]	43 (35.5) [121]	10 (20.8)	33 (45.2)	0.0061[a]
Low HDL cholesterol, *n* (%)	19 (14.7) [129]	4 (7.3)	15 (20.3)	0.0463[a]	18 (14.9) [121]	2 (4.2)	16 (21.9)	0.0081[a]

CKD, chronic kidney disease; Cre, creatinine; eGFR, estimated glomerular filtration rate; HDL, high-density lipoprotein; htTKV, height-adjusted total kidney volume; mutation position (cDNA), the location number of *PKD1* or *PKD2* mutation position in the nucleotide sequence of cDNA; NA, not applicable; PKD, polycystic kidney disease; TKV, total kidney volume; U-Prot, urinary protein excretion.

[a] $P < 0.05$.

Continuous values are expressed as the mean ± SD or median (minimum–maximum). Count data are expressed as n (%). Values for number of subjects are in brackets.

Table 2. Sex-adjusted and multivariable logistic regression for correlations between the TKV ≥1000 ml and risk factors (entire cohort, $N = 129$)

Variables A. Sex-adjusted logistic regression analyses	Model for *PKD1* truncating mutation ($R^2 = 0.08$, AUC = 0.68)		Model for *PKD1* splicing/ frameshift mutation ($R^2 = 0.10$, AUC = 0.70)		Model for *PKD1* nonsense mutation ($R^2 = 0.07$, AUC = 0.66)		Model for *PKD1* substitution ($R^2 = 0.07$, AUC = 0.66)	
	Odds ratio (95% CI)	*P* value	Odds ratio (95% CI)	*P* value	Odds ratio (95% CI)	*P* value	Odds ratio (95% CI)	*P* value
Men (vs. women)	3.59 (1.67–7.71)	0.0001[a]	3.56 (1.64–7.76)	0.0014[a]	3.65 (1.71–7.83)	0.0008[a]	3.59 (1.67–7.69)	0.0010[a]
PKD1 truncating mutation (vs. no)	1.61 (0.77–3.36)	0.2057	—	—	—	—	—	—
PKD1 splicing mutation or frameshift mutation (vs. no)	—	—	3.09 (1.23–7.76)	0.0165[a]	—	—	—	—
PKD1 nonsense mutation (vs. no)	—	—	—	—	0.85 (0.35–2.03)	0.7115	—	—
PKD1 substitution (vs. no)	—	—	—	—	—	—	0.74 (0.31–1.79)	0.5048

B. Multivariable logistic regression analyses	Model for *PKD1* truncating mutation ($R^2 = 0.15$, AUC = 0.75)		Model for *PKD1* splicing/ frameshift mutation ($R^2 = 0.17$, AUC = 0.77)		Model for *PKD1* nonsense mutation ($R^2 = 0.15$, AUC = 0.76)		Model for *PKD1* substitution ($R^2 = 0.15$, AUC = 0.75)	
	Odds ratio (95% CI)	*P* value	Odds ratio (95% CI)	*P* value	Odds ratio (95% CI)	*P* value	Odds ratio (95% CI)	*P* value
Men (vs. women)	1.84 (0.76–4.45)	0.1771	1.88 (0.77–4.61)	0.1685	1.82 (0.75–4.40)	0.1826	1.82 (0.75–4.39)	0.1843
Hypertension (vs. no)	3.01 (1.29–7.00)	0.0107[a]	3.00 (1.27–7.09)	0.0122[a]	3.21 (1.37–7.53)	0.0074[a]	3.09 (1.33–7.18)	0.0087[a]
Hyperuricemia (vs. no)	1.99 (0.73–5.41)	0.1777	1.91 (0.70–5.26)	0.2081	2.14 (0.79–5.77)	0.1346	2.01 (0.74–5.45)	0.1713
Low high-density lipoprotein cholesterol (vs. no)	1.82 (0.49–6.71)	0.3675	1.69 (0.45–6.32)	0.4386	1.68 (0.46–6.15)	0.4338	1.83 (0.50–6.75)	0.3634
PKD1 truncating mutation (vs. no)	1.36 (0.62–2.99)	0.4377	—	—	—	—	—	—
PKD1 splicing mutation or frameshift mutation (vs. no)	—	—	2.69 (1.02–7.10)	0.0454[a]	—	—	—	—
PKD1 nonsense mutation (vs. no)	—	—	—	—	0.69 (0.27–1.76)	0.4308	—	—
PKD1 substitution (vs. no)	—	—	—	—	—	—	0.79 (0.31–2.03)	0.6262

AUC, area under the receiver operating characteristic curve; PKD, polycystic kidney disease; R^2, McFadden's pseudo-*R*-squared; TKV, total kidney volume.
[a] $P < 0.05$.
Each mutation type, hypertension, hyperuricemia, and low high-density lipoprotein cholesterol were included in the multivariable model.

0.05. All statistical analyses were performed using JMP Pro version 15.0.0 software program (SAS Institute, Cary, NC).

RESULTS

Patient Characteristics

The characteristics of the entire patient group are found in Table 1 and Supplementary Table S1. Regarding mutation type, 34 patients harbored *PKD1* splicing mutations or frameshift mutations owing to the insertion or deletion of nucleotides (26.4%), 29 patients harbored *PKD1* nonsense mutations (22.5%), and 28 patients harbored *PKD1* substitutions (21.7%). At the time of evaluating TKV ≥ 1000 ml/ Mayo imaging classification, the median age was 45 years (minimum–maximum, 15–77 years), eGFR was 52.2 ± 29.4 ml/min per 1.73 m^2, TKV was 1525.0 ± 1161.1 ml, and maximum liver cyst diameter was 3.95 ± 3.55 cm. Hypertension affected 81 patients (62.8%).

Comparative analysis of the patients within the group revealed that 85.9% of the patients with TKV ≥1000 ml had a higher Mayo image classification (Mayo1C–1E) ($P < 0.0001$), compared with those with TKV < 1000 ml (24.0%). Furthermore, we determined the following characteristics: male sex (55.4% in patients with TKV ≥ 1000 ml vs. 25.5% in patients with TKV < 1000 ml, $P = 0.0007$), *PKD1* splicing mutation or frameshift mutation (35.1% in patients with TKV ≥1000 ml vs. 14.6% in patients with TKV <1000 ml, $P = 0.0087$), intracranial aneurysm (23.0% in patients with TKV ≥1000 ml vs. 3.6% in patients with TKV <1000 ml, $P = 0.0021$), hypertension (78.4% in patients with TKV ≥1000 ml vs. 41.8% in patients with TKV < 1000 ml, $P < 0.0001$), hyperuricemia (47.3% in patients with TKV ≥1000 ml vs. 16.4% in patients with TKV <1000 ml, $P = 0.0002$), and low HDL cholesterol (20.3% in patients with TKV ≥1000 ml vs. 7.3% in patients with TKV <1000 ml, $P = 0.0463$).

Drawing a comparative analysis between the patients with and without a Mayo classification of 1C–1E revealed that 83.6% of patients with Mayo classes 1C–1E compared with 20.8% of those with Mayo classes 1A–1B had higher rates of TKV ≥ 1000 ml ($P < 0.0001$). We also determined the following characteristics: male sex (50.7% in patients with Mayo 1C–1E vs. 31.3% in patients with Mayo 1A–1B, $P = 0.0346$), *PKD1* splicing mutations or frameshift mutations (35.6% in patients with Mayo 1C–1E vs. 14.6% in patients with Mayo 1A–1B, $P = 0.0110$), intracranial aneurysm (21.9% in patients with Mayo 1C–1E vs. 6.3% in patients with Mayo 1A–1B, $P = 0.0224$),

Table 3. Sex-adjusted and multivariable logistic regression analyses for correlations between the Mayo imaging classification 1C–1E and mutation types (entire cohort, $N = 121$)

Variables A. Sex-adjusted logistic regression analyses	Model for *PKD1* truncating mutation ($R^2 = 0.04$, AUC = 0.63)		Model for *PKD1* splicing/ frameshift mutation ($R^2 = 0.07$, AUC = 0.67)		Model for *PKD1* nonsense mutation ($R^2 = 0.03$, AUC = 0.60)		Model for *PKD1* substitution ($R^2 = 0.03$, AUC = 0.60)	
	Odds ratio (95% CI)	*P* value	Odds ratio (95% CI)	*P* value	Odds ratio (95% CI)	*P* value	Odds ratio (95% CI)	*P* value
Men (vs. women)	2.21 (1.03–4.78)	0.0430[a]	2.21 (1.01–4.83)	0.0474[a]	2.27 (1.06–4.89)	0.0353[a]	2.26 (1.05–4.86)	0.0366[a]
PKD1 truncating mutation (vs. no)	1.69 (0.80–3.57)	0.1700	—	—	—	—	—	—
PKD1 splicing mutation or frameshift mutation (vs. no)	—	—	3.17 (1.23–8.17)	0.0169[a]	—	—	—	—
PKD1 nonsense mutation (vs. no)	—	—	—	—	0.89 (0.37–2.17)	0.6912	—	—
PKD1 substitution (vs. no)	—	—	—	—	—	—	1.00 (0.41–2.44)	0.9945

B. Multivariable logistic regression analyses	Model for *PKD1* truncating mutation ($R^2 = 0.10$, AUC = 0.70)		Model for *PKD1* splicing/frameshift mutation ($R^2 = 0.12$, AUC = 0.74)		Model for *PKD1* nonsense mutation ($R^2 = 0.10$, AUC = 0.69)		Model for *PKD1* substitution ($R^2 = 0.10$, AUC = 0.68)	
	Odds ratio (95% CI)	*P* value	Odds ratio (95% CI)	*P* value	Odds ratio (95% CI)	*P* value	Odds ratio (95% CI)	*P* value
Men (vs. women)	1.31 (0.53–3.23)	0.5625	1.35 (0.54–3.39)	0.5165	1.27 (0.52–3.12)	0.5980	1.27 (0.52–3.11)	0.6039
Hypertension (vs. no)	1.67 (0.71–3.97)	0.2423	1.72 (0.72–4.13)	0.2230	1.80 (0.76–4.27)	0.1847	1.76 (0.75–4.15)	0.1967
Hyperuricemia (vs. no)	1.75 (0.65–4.71)	0.2669	1.66 (0.61–4.50)	0.3219	1.89 (0.71–5.02)	0.2013	1.88 (0.70–5.03)	0.2081
Low high-density lipoprotein cholesterol (vs. no)	4.85 (1.01–23.35)	0.0487[a]	4.56 (0.94–22.23)	0.0602	4.58 (0.96–21.91)	0.0570	4.66 (0.97–22.36)	0.0543
PKD1 truncating mutation (vs. no)	1.49 (0.68–3.29)	0.3230	—	—	—	—	—	—
PKD1 splicing mutation or frameshift mutation (vs. no)	—	—	2.84 (1.06–7.59)	0.0378[a]	—	—	—	—
PKD1 nonsense mutation (vs. no)	—	—	—	—	0.83 (0.32–2.12)	0.6912	—	—
PKD1 substitution (vs. no)	—	—	—	—	—	—	1.04 (0.40–2.65)	0.9425

AUC, area under the receiver operating characteristic curve; PKD, polycystic kidney disease; R^2, McFadden's pseudo-*R*-squared.
[a]$P < 0.05$.
Each mutation type, hypertension, hyperuricemia, and low high-density lipoprotein cholesterol were included in the multivariable model.

hypertension (74.0% in patients with Mayo 1C–1E vs. 52.1% in patients with Mayo 1A–1B, $P = 0.0133$), hyperuricemia (45.2% in patients with Mayo 1C–1E vs. 20.8% in patients with Mayo 1A–1B, $P = 0.0061$), and low HDL cholesterol (21.9% in patients with Mayo 1C–1E vs. 4.2% in patients with Mayo 1A–1B, $P = 0.0081$).

PKD1 Splicing/Frameshift Mutation as a Predictive Indicator of Both TKV ≥ 1000 ml and Mayo 1C–1E

Univariable and multivariable logistic regression analyses were performed for TKV ≥ 1000 ml and Mayo imaging classification 1C–1E (univariable analyses, Supplementary Tables S2 and S3; multivariable analyses, Tables 2 and 3). *PKD1* or *PKD2* mutation positions were not associated with TKV ≥ 1000 ml/Mayo 1C–1E (Supplementary Tables S2 and S3).

Among the mutation types, only the *PKD1* splicing/frameshift mutation had significant associations with TKV ≥ 1000 ml in sex-adjusted ($P = 0.0165$) and multivariable ($P = 0.0454$) logistic analyses (Figure 1a and Table 2). Similarly, only the *PKD1* splicing/frameshift mutation was significantly associated with Mayo 1C–1E in sex-adjusted ($P = 0.0169$) and multivariable ($P = 0.0378$) logistic analyses (Figure 1b and Table 3). In contrary, *PKD1* truncating mutation, *PKD1* nonsense mutation, and *PKD1* substitution had no significant associations with TKV ≥ 1000 ml/Mayo 1C–1E in sex-adjusted and multivariable logistic analyses (Figure 1 and Tables 2–3).

DISCUSSION

Chronic kidney disease, especially hereditary kidney disease, results in a lifelong fight against illness. Therefore, we believe that providing useful predictive information to patients fighting this illness is important. Recently, the significance of a detailed mutation type for patients with ADPKD regarding cerebral

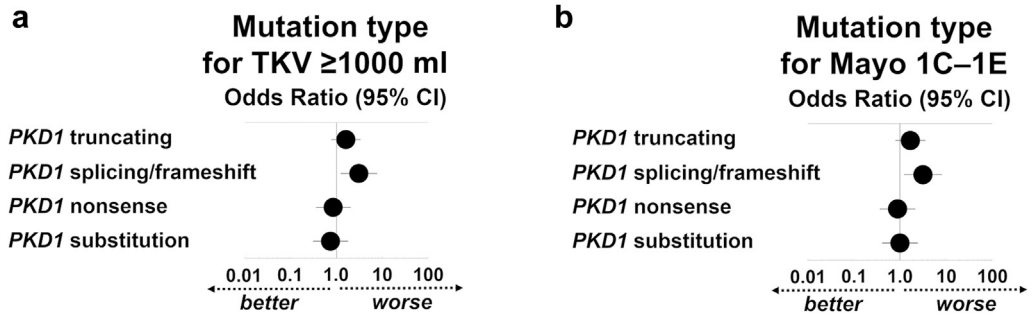

Figure 1. Odds ratios for TKV ≥ 1000 ml and the Mayo imaging classification 1C–1E in the entire cohort. (a) Mutation type for TKV ≥ 1000 ml. (b) Mutation type for the Mayo imaging classification 1C–1E. The circles represent odds ratios, and the bars represent 95% CI for the association of mutation types with TKV ≥ 1000 ml (derived from A in Table 2) and Mayo imaging classification 1C–1E (derived from A in Table 3). PKD, polycystic kidney disease; *PKD1* nonsense, *PKD1* nonsense mutation; *PKD1* splicing/frameshift, *PKD1* splicing mutation or *PKD1* frameshift mutation owing to the insertion or deletion of nucleotides; TKV, total kidney volume.

aneurysm, severity of polycystic liver disease,[32] and renal prognosis[33] has been reported. Nevertheless, the association between TKV/Mayo classification and germline mutation types has not been clearly elucidated. To the best of our knowledge, the present study is the first of its kind to perform a detailed analysis of patients with ADPKD, whereby the association between TKV ≥ 1000 ml/Mayo 1C–1E and genetic factors, including genotype, mutation type, and mutation position, was investigated. The results have revealed that the detailed mutation type of *PKD1* splicing/frameshift had a significant association with TKV ≥ 1000 ml and the Mayo 1C–1E classification.

As intrafamilial phenotypic variability exists among patients with the same mutation, somatic inactivation of the remaining wild-type *PKD1* or *PKD2* allele is thought to be required to initiate ADPKD and to play a key role in patients with ADPKD (the 2-hit model of ADPKD).[38–40] As a result, most previous studies on ADPKD have focused on the second hit mechanism and have made remarkable progress in the genome studies of ADPKD; however, research on germline mutations or genetic background has not progressed extensively. Although the 2-hit model is an important mechanism of ADPKD, recent evidence has suggested that PKD progression or severity is influenced by the level of functional polycystins (haploinsufficiency/loss of function model).[41,42]

In human genetic diseases, haploinsufficiency or loss of function is caused by the nonsense-mediated decay (NMD) process.[43–45] The degradation of transcripts containing premature termination codons through NMD[46–48] prevents the synthesis of aberrantly truncated proteins with potentially harmful dominant-negative effects.[49–51] Nevertheless, various additional determinants of NMD have been recently proposed[52,53]; NMD efficacy and escape from NMD have been attracting research attention.[52,54] It is possible that premature termination codon-containing mRNAs escaping NMD produce aberrant transcripts/truncated proteins with dominant-negative effects/gain of function that in turn contribute to phenotypic variation.[47,55,56]

In this study, TKV ≥ 1000 ml/Mayo 1C–1E had associations with *PKD1* splicing/frameshift mutations, which was not observed in patients with *PKD1* nonsense mutations (Figure 1). Transcripts with germline frameshift mutations and splicing mutations that escape NMD are reported in various genetic diseases[56–59] and experimental researches.[60–62] These transcripts can substantially change the amino acid sequences of the encoded proteins, exert a more dramatic effect on the protein 3-dimensional structure than a single amino acid change,[63,64] and form aberrant transcripts of the mutated genes.[56,57,65] In contrast, nonsense mutations that generate in-frame premature termination codons generally do not produce transcripts with extra aberrant amino acids and tend to cause haploinsufficiency/loss of function.[56,66] Indeed, Malan *et al*.[56] elucidated the phenotypic difference between Marshall-Smith Syndrome and Sotos-like overgrowth syndrome based on the difference between nonsense mutations/large deletions and frameshift/splice-site mutations. Patients with Marshall-Smith Syndrome had expression of both the normal and mutant alleles, indicating transcripts with frameshift and splice-site mutations that escape the NMD yield mutant proteins that exert a dominant-negative effect and cause a more severe phenotype of Marshall-Smith Syndrome. In contrast, patients with Sotos-like overgrowth syndrome had expression of only a single wild-type allele. This indicated that transcripts with large deletions and nonsense mutations undergoing NMD lead to haploinsufficiency in patients with Sotos-like overgrowth syndrome with mild intellectual deficits.[65] We consider that a similar underlying mechanism affected the patients with ADPKD in this study, resulting in no association between nonsense mutations

Table 4. Relationship between mutation types and phenotypes in kidney cysts, liver cysts, and intracranial aneurysms

Mutation type	Kidney dysfunction[33]	Kidney cysts (the present study)	Liver cysts[32]	Intracranial aneurysms (submitted)
Splicing mutation	●	●		● (younger age)
Frameshift mutation	●	●		▲ (younger age)
Nonsense mutation			●	
Substitution				▲ (older age, low GFR)

GFR, glomerular filtration rate; ●, high risk; ▲, moderate risk.

and TKV ≥ 1000 ml/Mayo 1C–1E. The phenotypic difference according to mutation type in patients with ADPKD (illustrated in in Table 4) might be affected by haploinsufficiency/loss of function model or dominant-negative effects/gain of function.

The present study has certain limitations. First, as an observational study, the causal relationships associated with our observations were not proven. Second, the sample size was relatively small; hence, further studies are required to confirm our findings in a larger patient cluster. Third, our results do not necessarily exclude a second-hit theory by somatic mutations. Nevertheless, the results of the present study suggest that the pathology of ADPKD can also develop when germline mutations are present. Genetic diagnosis can improve the clinical management of patients and has the potential to benefit patients with ADPKD (especially for a high-risk group of children, such as those with young-onset hypertension) by providing novel therapeutic options.[67,68]

In conclusion, this study revealed that patients with ADKPD exhibited an association between *PKD1* splicing mutations or *PKD1* frameshift mutations and TKV ≥ 1000 ml and Mayo classification of 1C–1E. The novel finding that the differences in these germline mutations affect the severity of kidney cysts may provide prognostic benefits for patients with ADPKD.

DISCLOSURE

TM and KT report receiving travel fees and honoraria for lectures from Otsuka Pharmaceutical Co. TM and HK belong to an endowed department sponsored by Otsuka Pharmaceutical Co., Chugai Pharmaceutical Co., Kyowa Hakko Kirin Co., and JMS Co. All the other authors declared no competing interests.

ACKNOWLEDGMENTS

This study was supported in part by JSPS KAKENHI grant number JP 15K09279 and by a Grant-in-Aid for Intractable Renal Diseases Research, Research on rare and intractable diseases, Health and Labour Sciences Research Grants from the Ministry of Health, Labour and Welfare of Japan.

SUPPLEMENTARY MATERIAL

Supplementary File (PDF)

Supplementary Methods. Mutation analysis, classification of mutation types, and classification of mutation positions; measurement of maximum liver cyst diameter, total kidney volume, maximum kidney cyst, and intracranial aneurysms; definitions of comorbidities.

Figure S1. Patient selection flowchart.

Table S1. Patient characteristics according to TKV and Mayo classification (entire cohort, n = 129).

Table S2. Univariable logistic regression analyses for correlations between the TKV ≥ 1000 ml and risk factors (entire cohort and subcohorts).

Table S3. Univariable logistic regression analyses for correlations between the Mayo imaging classification 1C–1E and risk factors (entire cohort and subcohorts).

REFERENCES

1. Mochizuki T, Tsuchiya K, Nitta K. Autosomal dominant polycystic kidney disease: recent advances in pathogenesis and potential therapies. *Clin Exp Nephrol*. 2013;17:317–326. https://doi.org/10.1007/s10157-012-0741-0
2. Ushio Y, Kataoka H, Sato M, et al. Association between anemia and renal prognosis in autosomal dominant polycystic kidney disease: a retrospective study. *Clin Exp Nephrol*. 2020;24:500–508. https://doi.org/10.1007/s10157-020-01856-1
3. Uchiyama K, Mochizuki T, Shimada Y, et al. Factors predicting decline in renal function and kidney volume growth in autosomal dominant polycystic kidney disease: a prospective cohort study (Japanese Polycystic Kidney Disease registry: J-PKD). *Clin Exp Nephrol*. 2021;25:970–980. https://doi.org/10.1007/s10157-021-02068-x
4. Grantham JJ, Torres VE. The importance of total kidney volume in evaluating progression of polycystic kidney disease. *Nat Rev Nephrol*. 2016;12:667–677. https://doi.org/10.1038/nrneph.2016.135
5. Perrone RD, Mouksassi MS, Romero K, et al. Total kidney volume is a prognostic biomarker of renal function decline and progression to end-stage renal disease in patients with autosomal dominant polycystic kidney disease [published correction appears in *Kidney Int Rep*. 2018;3:1015]. *Kidney Int Rep*. 2017;2:442–450. https://doi.org/10.1016/j.ekir.2017.01.003
6. Tangri N, Hougen I, Alam A, Perrone R, McFarlane P, Pei Y. Total kidney volume as a biomarker of disease progression in autosomal dominant polycystic kidney disease. *Can J Kidney Health Dis*. 2017;4:2054358117693355. https://doi.org/10.1177/2054358117693355
7. Irazabal MV, Rangel LJ, Bergstralh EJ, et al. Imaging classification of autosomal dominant polycystic kidney disease: a simple model for selecting patients for clinical trials. *J Am Soc Nephrol*. 2015;26:160–172. https://doi.org/10.1681/ASN.2013101138

8. Chebib FT, Perrone RD, Chapman AB, et al. A practical guide for treatment of rapidly progressive ADPKD with tolvaptan. *J Am Soc Nephrol*. 2018;29:2458–2470. https://doi.org/10.1681/ASN.2018060590
9. Gansevoort RT, Arici M, Benzing T, et al. Recommendations for the use of tolvaptan in autosomal dominant polycystic kidney disease: a position statement on behalf of the ERA-EDTA Working Groups on Inherited Kidney Disorders and European Renal Best Practice. *Nephrol Dial Transplant*. 2016;31:337–348. https://doi.org/10.1093/ndt/gfv456
10. Brosnahan GM, Abebe KZ, Moore CG, et al. Patterns of kidney function decline in autosomal dominant polycystic kidney disease: a post hoc analysis from the HALT-PKD trials. *Am J Kidney Dis*. 2018;71:666–676. https://doi.org/10.1053/j.ajkd.2017.10.023
11. Grantham JJ, Torres VE, Chapman AB, et al. Volume progression in polycystic kidney disease. *N Engl J Med*. 2006;354:2122–2130. https://doi.org/10.1056/NEJMoa054341
12. Bhutani H, Smith V, Rahbari-Oskoui F, et al. A comparison of ultrasound and magnetic resonance imaging shows that kidney length predicts chronic kidney disease in autosomal dominant polycystic kidney disease. *Kidney Int*. 2015;88:146–151. https://doi.org/10.1038/ki.2015.71
13. Torres VE, Chapman AB, Devuyst O, et al. Tolvaptan in patients with autosomal dominant polycystic kidney disease. *N Engl J Med*. 2012;367:2407–2418. https://doi.org/10.1056/NEJMoa1205511
14. Gimpel C, Bergmann C, Mekahli D. The wind of change in the management of autosomal dominant polycystic kidney disease in childhood. *Pediatr Nephrol*. Published online March 7, 2021. https://doi.org/10.1007/s00467-021-04974-4
15. Marlais M, Cuthell O, Langan D, Dudley J, Sinha MD, Winyard PJ. Hypertension in autosomal dominant polycystic kidney disease: a meta-analysis. *Arch Dis Child*. 2016;101:1142–1147. https://doi.org/10.1136/archdischild-2015-310221
16. Cadnapaphornchai MA, George DM, McFann K, et al. Effect of pravastatin on total kidney volume, left ventricular mass index, and microalbuminuria in pediatric autosomal dominant polycystic kidney disease. *Clin J Am Soc Nephrol*. 2014;9:889–896. https://doi.org/10.2215/CJN.08350813
17. Cho Y, Tong A, Craig JC, et al. Establishing a core outcome set for autosomal dominant polycystic kidney disease: report of the standardized outcomes in nephrology-polycystic kidney disease (SONG-PKD) consensus workshop. *Am J Kidney Dis*. 2021;77:255–263. https://doi.org/10.1053/j.ajkd.2020.05.024
18. The polycystic kidney disease 1 gene encodes a 14-kb transcript and lies within a duplicated region on chromosome 16. The European Polycystic Kidney Disease Consortium [published correction appears in *Cell*. 1994;78:725]. *Cell*. 1994;77:881–894. https://doi.org/10.1016/0092-8674(94)90137-6
19. Mochizuki T, Wu G, Hayashi T, et al. PKD2, a gene for polycystic kidney disease that encodes an integral membrane protein. *Science*. 1996;272:1339–1342. https://doi.org/10.1126/science.272.5266.1339
20. Hateboer N, v Dijk MA, Bogdanova N, et al. Comparison of phenotypes of polycystic kidney disease types 1 and 2. European PKD1-PKD2 Study Group. *Lancet*. 1999;353:103–107. https://doi.org/10.1016/s0140-6736(98)03495-3
21. Cornec-Le Gall E, Audrézet MP, Chen JM, et al. Type of PKD1 mutation influences renal outcome in ADPKD. *J Am Soc Nephrol*. 2013;24:1006–1013. https://doi.org/10.1681/ASN.2012070650
22. Higashihara E, Horie S, Kinoshita M, et al. A potentially crucial role of the PKD1 C-terminal tail in renal prognosis. *Clin Exp Nephrol*. 2018;22:395–404. https://doi.org/10.1007/s10157-017-1477-7
23. Barua M, Cil O, Paterson AD, et al. Family history of renal disease severity predicts the mutated gene in ADPKD. *J Am Soc Nephrol*. 2009;20:1833–1838. https://doi.org/10.1681/ASN.2009020162
24. Cornec-Le Gall E, Audrézet MP, Renaudineau E, et al. PKD2-related autosomal dominant polycystic kidney disease: prevalence, clinical presentation, mutation spectrum, and prognosis. *Am J Kidney Dis*. 2017;70:476–485. https://doi.org/10.1053/j.ajkd.2017.01.046
25. Rossetti S, Burton S, Strmecki L, et al. The position of the polycystic kidney disease 1 (PKD1) gene mutation correlates with the severity of renal disease. *J Am Soc Nephrol*. 2002;13:1230–1237. https://doi.org/10.1097/01.asn.0000013300.11876.37
26. Harris PC, Bae KT, Rossetti S, et al. Cyst number but not the rate of cystic growth is associated with the mutated gene in autosomal dominant polycystic kidney disease. *J Am Soc Nephrol*. 2006;17:3013–3019. https://doi.org/10.1681/ASN.2006080835
27. Hwang YH, Conklin J, Chan W, et al. Refining genotype-phenotype correlation in autosomal dominant polycystic kidney disease. *J Am Soc Nephrol*. 2016;27:1861–1868. https://doi.org/10.1681/ASN.2015060648
28. Heyer CM, Sundsbak JL, Abebe KZ, et al. Predicted mutation strength of nontruncating PKD1 mutations aids genotype-phenotype correlations in autosomal dominant polycystic kidney disease. *J Am Soc Nephrol*. 2016;27:2872–2884. https://doi.org/10.1681/ASN.2015050583
29. Cornec-Le Gall E, Audrézet MP, Rousseau A, et al. The PROPKD score: A new algorithm to predict renal survival in autosomal dominant polycystic kidney disease. *J Am Soc Nephrol*. 2016;27:942–951. https://doi.org/10.1681/ASN.2015010016
30. Nobakht N, Hanna RM, Al-Baghdadi M, et al. Advances in autosomal dominant polycystic kidney disease: a clinical review. *Kidney Med*. 2020;2:196–208. https://doi.org/10.1016/j.xkme.2019.11.009
31. Rossetti S, Consugar MB, Chapman AB, et al. Comprehensive molecular diagnostics in autosomal dominant polycystic kidney disease. *J Am Soc Nephrol*. 2007;18:2143–2160. https://doi.org/10.1681/ASN.2006121387
32. Kataoka H, Watanabe S, Sato M, et al. Predicting liver cyst severity by mutations in patients with autosomal-dominant polycystic kidney disease. *Hepatol Int*. 2021;15:791–803. https://doi.org/10.1007/s12072-021-10176-9
33. Kataoka H, Fukuoka H, Makabe S, et al. Prediction of renal prognosis in patients with autosomal dominant polycystic kidney disease using PKD1/PKD2 mutations. *J Clin Med*. 2020;9:146. https://doi.org/10.3390/jcm9010146
34. Mochizuki T, Teraoka A, Akagawa H, et al. Mutation analyses by next-generation sequencing and multiplex ligation-dependent probe amplification in Japanese autosomal dominant

polycystic kidney disease patients. *Clin Exp Nephrol*. 2019;23:1022–1030. https://doi.org/10.1007/s10157-019-01736-3

35. Curtis MJ, Bond RA, Spina D, et al. Experimental design and analysis and their reporting: new guidance for publication in BJP [published correction appears in *Br J Pharmacol*. 2015;172:4600]. *Br J Pharmacol*. 2015;172:3461–3471. https://doi.org/10.1111/bph.12856
36. Vittinghoff E, McCulloch CE. Relaxing the rule of ten events per variable in logistic and Cox regression. *Am J Epidemiol*. 2007;165:710–718. https://doi.org/10.1093/aje/kwk052
37. Hauber AB, González JM, Groothuis-Oudshoorn CG, et al. Statistical methods for the analysis of discrete choice experiments: A report of the ISPOR conjoint analysis good research practices task force. *Value Health*. 2016;19:300–315. https://doi.org/10.1016/j.jval.2016.04.004
38. Qian F, Watnick TJ, Onuchic LF, Germino GG. The molecular basis of focal cyst formation in human autosomal dominant polycystic kidney disease type I. *Cell*. 1996;87:979–987. https://doi.org/10.1016/s0092-8674(00)81793-6
39. Pei Y, Watnick T, He N, et al. Somatic PKD2 mutations in individual kidney and liver cysts support a "two-hit" model of cystogenesis in type 2 autosomal dominant polycystic kidney disease. *J Am Soc Nephrol*. 1999;10:1524–1529. https://doi.org/10.1681/ASN.V1071524
40. Wu G, D'Agati V, Cai Y, et al. Somatic inactivation of Pkd2 results in polycystic kidney disease. *Cell*. 1998;93:177–188. https://doi.org/10.1016/s0092-8674(00)81570-6
41. Lantinga-van Leeuwen IS, Leonhard WN, van der Wal A, Breuning MH, de Heer E, Peters DJ. Kidney-specific inactivation of the Pkd1 gene induces rapid cyst formation in developing kidneys and a slow onset of disease in adult mice. *Hum Mol Genet*. 2007;16:3188–3196. https://doi.org/10.1093/hmg/ddm299
42. Hopp K, Ward CJ, Hommerding CJ, et al. Functional polycystin-1 dosage governs autosomal dominant polycystic kidney disease severity. *J Clin Invest*. 2012;122:4257–4273. https://doi.org/10.1172/JCI64313
43. Rio Frio T, Wade NM, Ransijn A, Berson EL, Beckmann JS, Rivolta C. Premature termination codons in PRPF31 cause retinitis pigmentosa via haploinsufficiency due to nonsense-mediated mRNA decay. *J Clin Invest*. 2008;118:1519–1531. https://doi.org/10.1172/JCI34211
44. Bateman JF, Freddi S, Nattrass G, Savarirayan R. Tissue-specific RNA surveillance? Nonsense-mediated mRNA decay causes collagen X haploinsufficiency in Schmid metaphyseal chondrodysplasia cartilage. *Hum Mol Genet*. 2003;12:217–225. https://doi.org/10.1093/hmg/ddg054
45. Nogueira G, Fernandes R, Garcia-Moreno JF, Romão L. Nonsense-mediated RNA decay and its bipolar function in cancer. *Mol Cancer*. 2021;20:72. https://doi.org/10.1186/s12943-021-01364-0
46. Kurosaki T, Maquat LE. Nonsense-mediated mRNA decay in humans at a glance. *J Cell Sci*. 2016;129:461–467. https://doi.org/10.1242/jcs.181008
47. Nguyen LS, Wilkinson MF, Gecz J. Nonsense-mediated mRNA decay: inter-individual variability and human disease. *Neurosci Biobehav Rev*. 2014;46:175–186. https://doi.org/10.1016/j.neubiorev.2013.10.016
48. Miller JN, Pearce DA. Nonsense-mediated decay in genetic disease: friend or foe? *Mutat Res Rev Mutat Res*. 2014;762:52–64. https://doi.org/10.1016/j.mrrev.2014.05.001
49. Anna A, Monika G. Splicing mutations in human genetic disorders: examples, detection, and confirmation [published correction appears in *J Appl Genet*. 2019;60:231]. *J Appl Genet*. 2018;59:253–268. https://doi.org/10.1007/s13353-018-0444-7
50. Nicholson P, Yepiskoposyan H, Metze S, Zamudio Orozco R, Kleinschmidt N, Mühlemann O. Nonsense-mediated mRNA decay in human cells: mechanistic insights, functions beyond quality control and the double-life of NMD factors. *Cell Mol Life Sci*. 2010;67:677–700. https://doi.org/10.1007/s00018-009-0177-1
51. Khajavi M, Inoue K, Lupski JR. Nonsense-mediated mRNA decay modulates clinical outcome of genetic disease. *Eur J Hum Genet*. 2006;14:1074–1081. https://doi.org/10.1038/sj.ejhg.5201649
52. Litchfield K, Reading JL, Lim EL, et al. Escape from nonsense-mediated decay associates with anti-tumor immunogenicity. *Nat Commun*. 2020;11:3800. https://doi.org/10.1038/s41467-020-17526-5
53. Lindeboom RG, Supek F, Lehner B. The rules and impact of nonsense-mediated mRNA decay in human cancers. *Nat Genet*. 2016;48:1112–1118. https://doi.org/10.1038/ng.3664
54. Dyle MC, Kolakada D, Cortazar MA, Jagannathan S. How to get away with nonsense: mechanisms and consequences of escape from nonsense-mediated RNA decay. *Wiley Interdiscip Rev RNA*. 2020;11:e1560. https://doi.org/10.1002/wrna.1560
55. Coban-Akdemir Z, White JJ, Song X, et al. Identifying genes whose mutant transcripts cause dominant disease traits by potential gain-of-function alleles. *Am J Hum Genet*. 2018;103:171–187. https://doi.org/10.1016/j.ajhg.2018.06.009
56. Malan V, Rajan D, Thomas S, et al. Distinct effects of allelic NFIX mutations on nonsense-mediated mRNA decay engender either a Sotos-like or a Marshall–Smith syndrome. *Am J Hum Genet*. 2010;87:189–198. https://doi.org/10.1016/j.ajhg.2010.07.001
57. Fujiwara T, Takeda N, Hara H, et al. Distinct variants affecting differential splicing of TGFBR1 exon 5 cause either Loeys–Dietz syndrome or multiple self-healing squamous epithelioma. *Eur J Hum Genet*. 2018;26:1151–1158. https://doi.org/10.1038/s41431-018-0127-1
58. Khajavi M, Inoue K, Wiszniewski W, Ohyama T, Snipes GJ, Lupski JR. Curcumin treatment abrogates endoplasmic reticulum retention and aggregation-induced apoptosis associated with neuropathy-causing myelin protein zero-truncating mutants. *Am J Hum Genet*. 2005;77:841–850. https://doi.org/10.1086/497541
59. Inoue K, Khajavi M, Ohyama T, et al. Molecular mechanism for distinct neurological phenotypes conveyed by allelic truncating mutations. *Nat Genet*. 2004;36:361–369. https://doi.org/10.1038/ng1322
60. Ajiboye AS, Esopi D, Yegnasubramanian S, Denmeade SR. Androgen receptor splice variants are not substrates of nonsense-mediated decay. *Prostate*. 2017;77:829–837. https://doi.org/10.1002/pros.23323

61. Pastor F, Kolonias D, Giangrande PH, Gilboa E. Induction of tumour immunity by targeted inhibition of nonsense-mediated mRNA decay. *Nature*. 2010;465:227–230. https://doi.org/10.1038/nature08999

62. Lindeboom RGH, Vermeulen M, Lehner B, Supek F. The impact of nonsense-mediated mRNA decay on genetic disease, gene editing and cancer immunotherapy. *Nat Genet*. 2019;51:1645–1651. https://doi.org/10.1038/s41588-019-0517-5

63. López-Bigas N, Audit B, Ouzounis C, Parra G, Guigó R. Are splicing mutations the most frequent cause of hereditary disease? *FEBS Lett*. 2005;579:1900–1903. https://doi.org/10.1016/j.febslet.2005.02.047

64. Walsh S, Gösswein SS, Rump A, et al. Novel dominant-negative NR2F1 frameshift mutation and a phenotypic expansion of the Bosch-Boonstra-Schaaf optic atrophy syndrome. *Eur J Med Genet*. 2020;63:104019. https://doi.org/10.1016/j.ejmg.2020.104019

65. Schanze D, Neubauer D, Cormier-Daire V, et al. Deletions in the 3′ part of the NFIX gene including a recurrent Alu-mediated deletion of exon 6 and 7 account for previously unexplained cases of Marshall–Smith syndrome. *Hum Mutat*. 2014;35:1092–1100. https://doi.org/10.1002/humu.22603

66. Lek M, Karczewski KJ, Minikel EV, et al. Analysis of protein-coding genetic variation in 60,706 humans. *Nature*. 2016;536:285–291. https://doi.org/10.1038/nature19057

67. Bergmann C, Guay-Woodford LM, Harris PC, Horie S, Peters DJM, Torres VE. Polycystic kidney disease. *Nat Rev Dis Primers*. 2018;4:50. https://doi.org/10.1038/s41572-018-0047-y

68. Makabe S, Manabe S, Kataoka H, et al. Urinary aquaporin 2 as a potential indicator predicting tolvaptan response in patients with ADPKD. *Kidney Int Rep*. 2021;6:2436–2444. https://doi.org/10.1016/j.ekir.2021.06.033